Hepatic Free Cholesterol Accumulates in Obese, Diabetic Mice and Causes Non-Alcoholic Steatohepatitis

Derrick M Van Rooyen[1], **Claire Z Larter**[1], **W Geoffrey Haigh**[2], **Matthew M Yeh**[3], **George Ioannou**[4], **Rahul Kuver**[2], **Sum P Lee**[2], **Narci C Teoh**[1], and **Geoffrey C Farrell**[1]

[1]Liver Research Group, ANU Medical School at The Canberra Hospital, Garran, ACT Australia

[2]Department of Gastroenterology, University of Washington, Seattle, WA, USA

[3]Department of Pathology, University of Washington Medical Centre, Seattle, WA 98195

[4]Veteran Affairs Puget Sound Health Care System, Seattle, WA

Abstract

Background & Aims—Type-2 diabetes and non-alcoholic steatohepatitis (NASH) are associated with insulin resistance and disordered cholesterol homeostasis. We investigated the basis for hepatic cholesterol accumulation with insulin resistance and its relevance to pathogenesis of NASH.

Methods—*Alms1* mutant (*foz/foz*) and wild-type (WT) NOD.B10 mice were fed high-fat diets that contained varying percentages of cholesterol; hepatic lipid pools and pathways of cholesterol turnover were determined. Hepatocytes were exposed to insulin concentrations that circulate in diabetic *foz/foz* mice.

Results—Hepatic cholesterol accumulation was attributed to up-regulation of low density lipoprotein receptor (LDLR) via activation of sterol regulatory element binding protein-2 (SREBP-2), reduced biotransformation to bile acids, and suppression of canalicular pathways for cholesterol and bile acid excretion in bile. Exposing primary hepatocytes to concentrations of insulin that circulate in diabetic *Alms1* mice replicated the increases in SREBP-2 and LDLR and suppression of bile salt export pump. Removing cholesterol from diet prevented hepatic accumulation of free cholesterol and NASH; increasing dietary cholesterol exacerbated hepatic accumulation of free cholesterol, hepatocyte injury or apoptosis, macrophage recruitment, and liver fibrosis.

Correspondence should be addressed to: Geoffrey C. Farrell (geoff.farrell@anu.edu.au); Gastroenterology and Hepatology Unit, The Canberra Hospital, Yamba Drive, Garran, ACT 2605, Australia. Ph: 612 6244 2473; Fax: 612 6244 3235.

No conflicts to disclose.

Conclusions—In obese, diabetic mice, hyperinsulinemia alters nuclear transcriptional regulators of cholesterol homeostasis, leading to hepatic accumulation of free cholesterol; the resulting cytotoxicity mediates transition of steatosis to NASH.

Keywords

lipotoxicity; LRH-1; Bsep; liver damage; diabetes; mouse model; obesity

Introduction

Non-alcoholic fatty liver disease (NAFLD) is highly prevalent in all contemporary societies. It represents a pathological spectrum, across which the most common manifestation, simple steatosis (SS) rarely progresses to liver cirrhosis or hepatocellular carcinoma (HCC). However, ~25% of cases also exhibit substantial hepatocellular injury and inflammation, known as steatohepatitis (NASH), which causes liver fibrosis that can progress to cirrhosis, liver failure and HCC[1,2]. NASH is invariably linked to insulin resistance (IR) and hyperinsulinemia, and associates strongly with type 2 diabetes (~50% cases) and metabolic syndrome (85% of cases). The pathogenesis of NASH is now conceptualized as a response to lipotoxicity, but the lipotoxic molecule(s) involved have not been clarified. Currently most in favour are free fatty acids (FFA)[3], but two lipidomic studies have shown increased hepatic cholesterol in human NASH patients[4,5], while mechanistic studies have implicated free cholesterol (FC)[6], or macrophages activated by FC[7] in hepatocyte injury and liver inflammation.

We have previously characterized a line of obese, diabetic mice which simulate Alström syndrome, a monozygotic form of childhood obesity associated with T2D, NASH and cirrhosis[8]. After 12 weeks on a high-fat (HF) (0.2% cholesterol) diet, *Alms1* mutant (*foz/foz*) mice on NOD.B10 background develop hyperinsulinemia, diabetes, hypercholesterolemia, and hypoadiponectinemia, which changes precede or accompany transformation of steatosis to NASH[9]. In preliminary studies, we noted extraordinarily high hepatic total cholesterol levels in *foz/foz* mice with NASH but not in similar lines with SS. Further, there was no correlation with free fatty acids (FFA), diacylglycerides (DAG), or ceramide. We have now used liver samples from our earlier publication[9] to explore the temporal relationships between hepatic cholesterol fractions, and pathways of hepatic cholesterol turnover, including a focus on the transcriptional regulators of cholesterol and bile acid metabolism. We then tested whether insulin was responsible for some or all the observed changes by direct experiments in primary murine hepatocytes. Finally, we used dietary interventions to deplete or accentuate hepatic cholesterol stores, and demonstrated that hepatic free cholesterol (FC) accumulation is causally related to severity of NAFLD/NASH.

Methods

Animals and diets

All experiments were approved by the ANU Animal Experimentation Ethics Committee. Only female mice were used. *Foz/foz* (*Alms1* mutant) and WT littermates (8 wk old) were fed chow (5% fat, 67% carbohydrate, 19% protein, 0% cholesterol) or high-fat (HF) (23% fat, 45% carbohydrate, 20% protein, 0.2% cholesterol) diets (Specialty Feeds, Australia) *ad libitum* for 12 or 24 weeks. The first part of the present experiments used tissue from animals reported in an earlier study[9]. Group *n* values were as follows: 12 week WT chow and HFD (*n*=6), *foz/foz* chow (*n*=7) and HFD (*n*=10); 24 week mice, *n*=5/grp. In a second experiment, female *foz/foz* (*n*=8–9) and WT littermates (*n*=7–11) were fed HF diet containing 0.0, 0.2, or 2.0% (w/w) cholesterol 24-weeks. At experimental endpoints, mice were fasted (4 h), serum/tissues harvested.

Serum and hepatic lipid analyses

Serum biochemistry was assessed using automated techniques (Clinical Chemistry, ACT Pathology). Hepatic FFA, FC, and neutral (esterified) lipids were quantitated using high-performance liquid chromatography (HPLC), as described[10], and results normalized to wet liver weight (g).

Histological analyses

Blinded hematoxylin/eosin-stained liver sections were scored by a hepatopathologist (MMY), using the NAFLD activity score (NAS)[11]. Sirius red-stained liver sections were used to quantify collagen fibres by image analysis (ImageJ, Bethesda, MD).

Quantitative analysis of gene expression

Gene expression was quantified using real-time PCR as previously described[9]. Primers are presented in Supplementary Table 1.

Protein quantitation

Nuclear protein was extracted from liver tissue using NE-PER nuclear/cytoplasmic extraction (Thermo, Rockford IL). Nuclear or whole liver proteins were quantitated using antibodies in Supplementary Table 2. Enhanced chemiluminescence images were captured (LAS-4000, FujiFilm, Tokyo), quantitated (MultiGauge V3.0, FujiFilm), and values expressed relative to heat-shock protein-90 (HSP90) or TATA box-binding protein (TBP), and normalized to WT chow levels.

HMG-CoA reductase activity

HMGR activity was assessed in hepatic microsomes by a radiometric assay[12].

Immunohistochemistry

Tissue sections underwent antigen retrieval (10 mM sodium-citrate, pH 6.0), and antibody labeling (Supplementary Table 2) using IHC select DAB kit (Millipore, Billerica, MA). A minimum of 6 random high-power fields were quantitated for each section. Positive staining was normalized to number of hepatocyte nuclei.

Primary hepatocyte culture

Primary hepatocytes were isolated from 6-week old female WT mice[13], and seeded onto rat-tail collagen (Gibco, CA) coated plates (5 $\mu g/cm^2$). Hepatocytes were cultured in William's E containing 1% bovine serum albumin (Sigma-Aldrich, St Louis, MO) at ~6.5×10^4 viable cells/cm^2. For insulin studies, hepatocytes were grown (48 h) in the presence of bovine pancreatic insulin (Sigma-Aldrich) at concentrations of 0.2, 6.5, and 13.0 ng/ml, which corresponds to previously measured fasting serum insulin concentrations in WT and HF-fed *foz/foz* mice at 12- and 24-weeks, respectively[9].

Statistical analyses

Data (mean±SEM) were analyzed by analysis of variance (ANOVA), with Tukey post-hoc testing (SPSS V17.0, Chicago, IL). Histological assessments were analyzed using Kruskal-Wallis' test, and group comparisons with Mann-Whitney *U*-test. $P<0.05$ was considered significant.

Results

Changes in hepatic cholesterol fractions during development of NASH

As previously reported[9], hepatomegaly occurs in HF-fed *foz/foz* mice by week 12 of dietary intake, whereas liver weights remain normal in chow-fed *foz/foz* and WT groups. Following onset of diabetes in HF-fed *foz/foz* mice, steatosis evolves to NASH with fibrosis between 12 and 24 weeks of HF intake[9]. Further analysis showed that HF diet (which contains 0.2% cholesterol) increased hepatic cholesteryl ester (CE) fractions ~200-fold at 12 weeks, and a further ~50-fold by 24 weeks in *foz/foz* mice compared to diet-matched WT controls (*P*<0.0001, Figure 1A). Whereas hepatic free cholesterol (FC) increased in both HF-fed *foz/foz* and WT mice at 12 weeks (Figure 1B), values in WT mice returned to chow-fed controls by 24 weeks. At this time, when fibrotic NASH was established in HF-fed *foz/foz* mice, hepatic FC was significantly higher than in HF-fed WT mice (*P*=0.027). In this work, oxysterol metabolites could be detected in some samples, but generally were below the assay limit for quantitative detection and there was no evident differences between experimental groups.

The hepatic free cholesterol uptake pathway, LDLR, is increased in HF-fed *foz/foz* mice

Three pathways for hepatic cholesterol uptake are the scavenger receptor-B1 (SR-B1), the low-density lipoprotein receptor (LDLR) and cluster differentiation protein-36 (CD-36). We earlier reported up-regulation of CD-36 expression in HF-fed *foz/foz* mice with NASH[9]. In the present studies, SR-B1 was down-regulated in HF-fed *foz/foz* mice compared with HF-fed WT controls (*P*=0.03, Supplementary Figure 1A), but LDLR, the major transporter responsible for FC uptake, was significantly increased at both 12 and 24 weeks (*P*=0.001, Figure 1C). Immunohistochemistry (IHC) illustrated dramatic over-expression of LDLR in mice with NASH, characterized by an extension from physiological vascular endothelial localization to also include intense hepatocyte surface expression (Figure 1D). This differential regulation of LDLR is consistent with the proposal that an increase in LDLR FC uptake by hepatocytes contributes to the increased liver content of cholesterol in *foz/foz* mice with NASH.

Cholesterol esterification and hydrolysis genes are up-regulated in HF-fed *foz/foz* mice with NASH, but *de novo* cholesterol biosynthesis is not

In light of the hepatic accumulation of FC in obese, diabetic *foz/foz* mice, we investigated pathways responsible for the *de novo* synthesis of cholesterol, and for the dynamic relationship between CE and FC. By 12 weeks of HF-feeding, HMG-CoA reductase (HMGR) activity, the rate limiting step in cholesterol biosynthesis, appeared (NS) to increase in *foz/foz* mice, but by 24 weeks enzyme activity was reduced ~10-fold in both HF-fed *foz/foz* and WT mice compared to respective chow-fed controls (*P*<0.05, Figure 2A), consistent with the expected suppression of hepatic cholesterol synthesis by HF-feeding. While acyl-CoA cholesterol:cholesteryl transferase (ACAT)-2 protein increased at both 12- and 24-week time points in HF-fed *foz/foz* mice compared with dietary and genotype controls (*P*<0.0001, Figure 2B), favouring CE formation, the CE hydrolytic pathway, as reflected by cholesteryl ester hydrolase (CEH) mRNA levels, was also selectively up-regulated in mice with NASH (*P*<0.05, Figure 2C). The latter pathway could account for the selective increase in FC seen in HF-fed *foz/foz* mice at 24 weeks.

Pathways of cholesterol biotransformation and export are down-regulated in *foz/foz* mice with NASH

Because hepatic biotransformation of cholesterol into bile acids constitutes the major pathway of cholesterol catabolism, we used RT-PCR to detect and semiquantify transcripts

for all relevant genes; each is transcriptionally regulated[14–17]. Levels of cytochrome P450 (Cyp)7a1 mRNA, the rate-limiting step for 90% of bile acid (BA) production from cholesterol, were reduced in HF-fed *foz/foz* mice compared to dietary and genotype controls (*P*=0.02, Figure 2D). Transcripts of the alternative pathway, mediated by Cyp27a1, and subsidiary bile acid synthesis genes, Cyps 7b1 and 8b1, were similarly down-regulated (Supplementary Figure 1B,C,D). In addition, the hepatic canalicular BA export protein (Bsep), was substantially suppressed in HF-fed *foz/foz* mice compared with HF-fed WT mice (*P*=0.008, Figure 2E); IHC confirmed a distinct reduction in hepatocyte canalicular Bsep staining (Supplementary Figure 1E). Further, ATP-binding cassette (ABC) transporters G-5/8, which facilitate cholesterol efflux across the bile canalicular membrane, were both down-regulated; ABCG5 expression decreased in HF-fed *foz/foz* mice by 24 weeks compared with HF-fed WT mice (*P*<0.0001, Supplementary Figure 1F), while ABCG8 expression was profoundly suppressed (*P*<0.0001) at both 12- and 24 weeks (Figure 2F). The combined effects of reduced expression of Cyp7a1 and other bile acid synthetic genes, ABCG5/8, Bsep and other canalicular transporters (MRP-2, Mdr2 – data not shown), indicate that hepatic cholesterol biotransformation and direct and indirect (as bile acids) secretion into bile are profoundly impaired in *foz/foz* mice with NASH.

Nuclear regulators of cholesterol and bile acid homeostasis are perturbed in mice with NASH

Key nuclear receptors involved in regulation of hepatic cholesterol/oxysterol homeostasis include sterol-regulatory element binding protein-2 (SREBP-2), liver receptor homolog-1 (LRH-1), farnesoid-X receptor (FXR), and small heterodimeric partner (Shp). LDLR expression is a particular target of SREBP-2, nuclear abundance (activation) of which increased significantly in HF-fed *foz/foz* mice at 12 weeks (*P*=0.004, Figure 3A). Although levels dropped by 24 weeks, expression remained significantly higher in HF-fed *foz/foz* than in WT mice (*P*=0.004, Figure 3A).

LRH-1 is the principle regulator of SR-B1, Cyp7a1 and other bile acid-synthesizing Cyps, ABCG5 and −8, and Bsep, all strongly down-regulated in obese, diabetic *foz/foz* mice (Figure 2D,E,F). HF-feeding increased nuclear LRH-1 protein in WT mice, but failed to up-regulate this nuclear receptor in *foz/foz* mice (*P*<0.0001, Figure 3B); and LRH-1 mRNA levels actually fell (data not shown), consistent with the observed failure of LRH-1 to maintain appropriate expression of SR-B1, Cyp7a, ABC-G5/8, and Bsep. Bile acids stimulate FXR, which functions as a negative regulator of cholesterol biotransformation directly by suppression of Cyps 7a1 and 27a1, and indirectly, via activation of Shp[18]. Consistent with impairment of bile acid synthesis described earlier, FXR was down-regulated in HF-fed *foz/foz* mice at both 12- and 24-weeks (*P*<0.0001, Figure 3C). Conversely, Shp was significantly increased by HF-feeding in *foz/foz* mice at 12 and 24 weeks (*P*<0.0001, Figure 3D), whereas induction of Shp by HF diet in WT mice only occurred after 24 weeks, and to a lesser extent.

Insulin activates SREBP-2 and LDLR and suppresses LRH-1 and Bsep in primary murine hepatocytes

A key feature of NAFLD and diabetic hypercholesterolemia is hyperinsulinemia, resulting from IR[8,19]. We tested whether insulin concentrations that circulate in *foz/foz* mice are sufficient to dysregulate hepatic cholesterol homeostasis. Using concentrations that simulated HF-fed *foz/foz* mice at 12 and 24 weeks (i.e. 6.5 and 13 ng/mL, respectively)[9], insulin increased total cellular SREBP-2 expression (*P*<0.0001, Figure 4A,D) with concomitant induction of LDLR (*P*<0.0001, Figure 4B,D). LRH-1 mRNA was suppressed, as well as Bsep protein, without significant effect on FXR (results not shown), but a fall in Shp mRNA (Figure 4F). We also conducted control experiments on liver from: (a) mice fed

a methionine and choline deficient diet (which develop steatohepatitis with low serum insulin levels), and (b) mice exposed to carbon tetrachloride for 4 weeks. In neither case was LDLR up-regulated on hepatocytes (Supplementary Figure 2). These findings support the proposal that hyperinsulinemia is a key factor that alters hepatic cholesterol homeostasis by increasing nuclear SREBP-2 and LDLR, and lowering LRH-1 and Bsep expression in hepatocytes. However, insulin is unlikely to be the only mediator of disordered hepatic cholesterol metabolism since it is clearly not responsible for the observed increase in nuclear Shp in HF-fed *foz/foz* mice (Figure 3D vs. Figure 4F).

Dietary modulations of cholesterol content alter hepatic free cholesterol with resultant modulation of liver injury, apoptosis, macrophage recruitment and fibrogenesis in mice with NASH

If hepatic FC is a lipotoxic mediator of injury, inflammation, and fibrosis in NAFLD, changing hepatic levels of FC should alter the pathological phenotype of liver disease. To test this, we used the same composition of "HF diet" for each group and modified only its cholesterol content, from 0%, through 0.2% (as in all earlier experiments) to 2.0%. HF-fed *foz/foz* mice fed no cholesterol HF diet showed lower serum ALT at 24 weeks (259 ± 37 U/L) than those fed the 0.2% cholesterol HF (430 ± 26 U/L), while the 2.0% cholesterol group had even higher ALT (534 ± 58 U/L) ($P<0.0001$ between groups, Figure 5A). As reported by others[20], a minor increase in serum ALT was also observed in WT mice fed 2.0% cholesterol HF diet ($P=0.05$). Increasing dietary cholesterol significantly increased serum cholesterol ($P<0.05$, Supplementary Figure 3A), hepatic CE content ($P<0.05$, Figure 5B), and, most profoundly, FC ($P<0.05$, Figure 5C). Conversely, hepatic TG, monoacylglycerides and DAG fractions, did not increase further with increased dietary cholesterol, and did not fall with cholesterol restriction (Figure 5D,E). Hepatic FFA fractions showed no significant changes in total (Figure 5F), saturated (Sa)-, and monounsaturated (Mu)-FFA observed in *foz/foz* mice fed HF diet with varying cholesterol content (Supplementary Figure 3D,E). Similarly, while polyunsaturated FFA were consistently less in HF-fed *foz/foz* versus corresponding WT mice (Supplementary Figure 3F), there were no differences between cholesterol dietary groups of *foz/foz* mice, despite major differences in NASH severity.

In preliminary studies to assess the effects of dietary cholesterol content on the pathogenesis of NASH, we quantitated hepatocyte cell death and macrophage recruitment by IHC. Immunolabeling of the hepatic cytokeratin-18 (Ck-18) fragmentation product, M30, which accumulates in response to caspase-3 activation[21], showed that increasing cholesterol content from 0.2% to 2.0% increased cell death from $12 \pm 1\%$ of counted hepatocytes to $17\% \pm 0.4\%$ in HF diet-fed *foz/foz* mice, while absence of cholesterol reduced it to $4.5 \pm 1.0\%$ ($P<0.05$, Figure 6A). Similarly, increased F4/80 (macrophage) immmunostaining correlated with dietary cholesterol supplementation (Figure 6B). Compared with the no cholesterol-HF group, macrophage localization occurred around steatotic (cholesterol-loaded) hepatocytes in 0.2% and 2.0% cholesterol HF diet-fed *foz/foz* mouse livers (Figure 6C). These changes in injury/inflammatory markers were supported by histological scoring; there was identical (grade 3) steatosis in each HF-fed *foz/foz* group, but progressive increases in hepatocellular ballooning and inflammation in response to dietary cholesterol loading (Table 1). Finally, we quantified fibrotic severity of NASH by the density and pattern of Sirius red staining in *foz/foz* mice. This was least with cholesterol, intermediate in the 0.2% cholesterol and highest in the 2.0% cholesterol groups ($P<0.05$ vs. 0% cholesterol group, Figure 6D,E).

Discussion

While small studies of human NASH livers have found increased hepatic cholesterol content, data to establish the pathogenic basis for such cholesterol accumulation are restricted[4,5]. In the present studies, we first confirmed that hepatic FC accumulates in the *foz/foz* dietary and genetic model of obesity and diabetes-related NASH. We then resolved how this cholesterol accumulation is related to dysregulation of known pathways that regulate cholesterol homeostasis, with a key role for insulin resistance, the abnormality common to atherogenic dyslipidemia, T2D and NASH. Specifically, while hepatic cholesterol biosynthesis is suppressed (or normal), expression of the FC uptake transporter, LDLR, increases, and pathways for cholesterol biotransformation to form bile acids, and direct and indirect (via bile acids) secretion of cholesterol into bile are profoundly suppressed. A plausible explanation for this pattern of up-and down-regulated genes and proteins was activation of SREBP-2, and failure of LRH-1 expression to increase as occurred with WT mice that do not develop cholesterol accumulation or NASH. Exposing WT primary hepatocytes to the high concentrations of insulin that circulate in HF-fed *foz/foz* mice confirmed that hyperinsulinemia accounts for, at least in part, the observed dysregulation of hepatic cholesterol turnover by up-regulating SREBP-2 and LDLR, while simultaneously down-regulating LRH-1 gene expression and Bsep, as observed *in vivo*.

The genetic defect in *foz/foz* mice is an 11 base-pair deletion in *Alms1* resulting in a truncated Alms1 protein 1. Loss-of-function mutations (or deletions) in Alms1 cause Alström syndrome. Likewise, *Alms1* mutant mice develop obesity, T2D and dyslipidemia, all highly relevant to NASH pathogenesis. Alms1 protein localizes to the basal body of primary cilia, including those on hypothalamic neurons that are critical for appetite regulation. However, hepatocytes are one of few cell types that do not bear a primary cilium, so that Alms1 is unlikely to be involved directly in cholesterol turnover and NASH pathogenesis; indeed, *foz/foz* balb-c mice, which do not develop diabetes, also do not develop NASH (Larter, Yeh, Farrell – unpublished data). What is clear is that cholesterol homeostasis observed in these studies coincides with increases in circulating insulin levels that are not observed in chow-fed *foz/foz* mice with SS. Nonetheless, direct comparative studies of hepatocytes (lean and fat-loaded) from *Alms1* mutant mice are *in train*. It is also noted that patients with hypothalamic and pituitary disorders often have severe NASH[22], and it will be important to demonstrate that cholesterol accumulates in the liver in other models of NASH, as it does in the human condition[4], before concluding its general importance as a lipotoxic molecule in pathogenesis of NASH.

The increase in SREBP-2 activation observed here in diabetic mice with NASH is consistent with reported increases in both FC and SREBP-2 in human NASH[5]; this indicates an *inappropriate* SREBP-2 response to FC accumulation during NASH pathogenesis. Importantly, Xie *et al.*[23] demonstrated that insulin directly stimulates SREBP-2 expression, and we confirmed that 48h exposure of primary hepatocytes to the same concentrations of insulin that circulate in these obese, diabetic *foz/foz* mice induce both SREBP-2 and LDLR, as well as suppressing LRH-1 and Bsep gene expression. The present results therefore provide an explanation for the previously unexplained findings showing that insulin resistance (more specifically, hyperinsulinemia) can lead to prolonged, intense non-physiological expression of the hepatic FC uptake transporter, LDLR, at a time that hepatic cholesterol stores are already increased. However, other factors must also play a role in overall cholesterol homeostasis, as HMGR activity was suppressed in *foz/foz* mice with NASH, the expected response to FC accumulation, and FXR transcripts were also suppressed in the tissue studies, and by insulin in primary hepatocytes.

Regulation of hepatic cholesterol turnover also includes control of biotransformation to form primary bile acids, and export pathways, all largely regulated by LRH-1. LRH-1 mRNA levels were suppressed by insulin in isolated hepatocytes (Figure 4E), and HF-feeding (associated with hyperinsulinemia in this model) failed to increased nuclear LRH-1 in *foz/foz* mice, as it clearly did in HF-fed WT mice (Figure 3B). LRH-1 controls expression of ABCG5/8, Bsep, Cyps 7a1/27a1/7b1/8a1, and SR-B1[24–27], all down-regulated in *foz/foz* mice with NASH. This appears to be the first evidence that an abrogated LRH-1 response (i.e. failure to increase) could be pertinent to NASH pathogenesis, and our observations in lean murine hepatocytes indicate that the high insulin levels in cholesterol-loaded hepatocytes could counter what might otherwise be an adaptive increase to FC accumulation.

While our studies found lowered HMGR activity in HF-fed *foz/foz* and WT mice after 24 weeks, chow-fed *foz/foz* mice appeared to show increased HMGR activity. These data do not exclude a role for *de novo* biosynthesis of cholesterol as contributing to NASH pathogenesis in its earlier stages, but it does not appear to be the major pathway to continuing cholesterol accumulation at the later stages. Under physiological conditions, most hepatic cholesterol is biotransformed to bile acids via the Cyp7a1-dependent pathway (Cyps 27a1, 7b1, 8a1 play minor or subsidiary roles). In turn, residual FC and bile acids are pumped across the canalicular membrane via several ABC transporters, including ABCG5/8, and Bsep. The most profound changes in pathways of hepatic cholesterol turnover in our model of NASH were suppression of these genes and proteins that mediate cholesterol biotransformation, and biliary cholesterol and BA excretion. We have not excluded a role for other nuclear receptors in the effects on BA formation and bile secretion, and note that there was a discrepancy between FXR mRNA levels suppressed in tissue and *in vitro* experiments, and FXR nuclear protein levels, which increase in HF-fed WT but not *foz/foz* mice. Conversely Shp, which is regulated by FXR, increased markedly in *foz/foz* mice. The reason for this apparent discrepancy requires further investigation.

Despite cholesterol being a known cytotoxic lipid in atherosclerotic plaque development[28], information about the role of cholesterol in the pathogenesis of NASH is more limited. One epidemiological study has shown a relationship between dietary cholesterol intake and risk of cirrhosis over 13 years[29]. Puri *et al*.[4] demonstrated significant increases in hepatic FC in human NAFLD, with higher levels observed in a small number of NASH patients, while hepatic FFA levels were similar between NASH and benign forms of NAFLD. Mari *et al*., using rodent liver, found that cholesterol loading of hepatocytes induced mitochondrial stress, and increased sensitivity to tumour necrosis factor (TNF) and Fas ligand (FasL)-induced cell death[6]. In the present study, increasing dietary cholesterol significantly increased serum ALT, hepatic apoptosis, macrophage recruitment, and fibrotic severity of NASH, while removing dietary cholesterol had the opposite, protective effects. Dietary cholesterol modulation also substantively influenced hepatic total and free cholesterol levels, providing the first clear evidence that in an insulin-resistant model, hepatic cholesterol loading directly affects hepatocyte apoptosis, liver inflammatory cell recruitment and fibrogenesis in NASH. Conversely, hepatic levels of TG, DAG, monoacylglycerides, and FFA, while generally elevated in HF-fed *foz/foz* mice compared with WT counterparts, were unchanged in relation to the modulated severity of NASH. Finally, while the size of the hepatic FC pool correlated with NASH severity during all 3 dietary interventions, we have not completely excluded a role for oxysterol metabolites, accumulation of which in this study challenged the limits of detection but appeared to be similar across experimental groups.

In summary, we have demonstrated that hepatic free cholesterol increases substantially in obese, insulin-resistant, diabetic mice, and levels correlate with histological severity of

NASH. Hyperinsulinemia is likely responsible for dysregulation of at least two hepatic nuclear receptors (SREBP-2, LRH-1), resulting, respectively, in increased LDLR expression on hepatocytes and profound down-regulation of cholesterol biotransformation and FC/BA efflux pathways in the liver. The resultant hepatic FC accumulation is directly related to the severity of liver injury, cell death by apoptosis, macrophage accumulation, and fibrosis in NASH. The therapeutic implications are to improve insulin sensitivity by restoring optimal levels of physical activity and reducing dietary sources and endogenous cholesterol synthesis, as is well known in diabetes prevention. Meanwhile, if cholesterol is as important in pathogenesis of human NASH as it clearly is in our model with similar metabolic risk factors, pharmacological inhibition of cholesterol absorption, recirculation and synthesis merits greater attention as potential therapy for NASH.

Supplementary Material

Refer to Web version on PubMed Central for supplementary material.

Acknowledgments

Abbreviations

CE	cholesteryl esters
Cyp7a1	7α-hydroxylase
FC	free cholesterol
FFA	free fatty acids
FXR	farnesoid X receptor
HMGR	3-hydroxy-3-methyl-glutaryl-CoA reductase
HPLC	high-performance liquid chromatography
IR	insulin resistant
LRH-1	liver-receptor homolog-1
MAG	monoacylglycerides
NAFLD	non-alcoholic fatty liver disease
NASH	non-alcoholic steatohepatitis
Shp	small heterodimer partner
SREBP	sterol regulatory element–binding protein
SS	simple steatosis
T2D	type-2 diabetes
TG	triglycerides

References

1. Harrison SA, Di Bisceglie AM. Advances in the understanding and treatment of nonalcoholic fatty liver disease. Drugs. 2003; 63:2379–94. [PubMed: 14609346]

2. Muddu AK, Guha IN, Elsharkawy AM, Mann DA. Resolving fibrosis in the diseased liver: translating the scientific promise to the clinic. Int. J. Biochem. Cell Biol. 2007; 39:695–714. [PubMed: 17110155]

3. Neuschwander-Tetri BA. Hepatic lipotoxicity and the pathogenesis of nonalcoholic steatohepatitis: the central role of nontriglyceride fatty acid metabolites. Hepatology. 2010; 52:774–88. [PubMed: 20683968]

4. Puri P, Baillie RA, Wiest MM, Mirshahi F, Choudhury J, Cheung O, Sargeant C, Contos MJ, Sanyal AJ. A lipidomic analysis of nonalcoholic fatty liver disease. Hepatology. 2007; 46:1081–90. [PubMed: 17654743]

5. Caballero F, Bataller R, Lacy A, Fernandez-Checa JC, Caballeria J, Garcia-Ruiz C. Enhanced free cholesterol, SREBP-2 and StAR expression in human NASH. J. Hepatol. 2009; 50:789–796. [PubMed: 19231010]

6. Mari M, Caballero F, Colell A, Morales A, Caballeria J, Fernandez A, Enrich C, Fernandez-Checa JC, Garcia-Ruiz C. Mitochondrial free cholesterol loading sensitizes to TNF- and Fas-mediated steatohepatitis. Cell Metab. 2006; 4:185–98. [PubMed: 16950136]

7. Bieghs V, Wouters K, van Gorp PJ, Gijbels MJ, de Winther MP, Binder CJ, Lutjohann D, Febbraio M, Moore KJ, van Bilsen M, Hofker MH, Shiri-Sverdlov R. Role of scavenger receptor A and CD36 in diet-induced nonalcoholic steatohepatitis in hyperlipidemic mice. Gastroenterology. 2010; 138:2477–86. 2486, e1–3. [PubMed: 20206177]

8. Arsov T, Larter CZ, Nolan CJ, Petrovski N, Goodnow CC, Teoh NC, Yeh MM, Farrell GC. Adaptive failure to high-fat diet characterizes steatohepatitis in *Alms1* mutant mice. Biochem. Biophys. Res. Commun. 2006; 342:1152–1159. [PubMed: 16516152]

9. Larter CZ, Yeh MM, Van Rooyen DM, Teoh NC, Brooling J, Hou JY, Williams J, Clyne M, Nolan CJ, Farrell GC. Roles of adipose restriction and metabolic factors in progression of steatosis to steatohepatitis in obese, diabetic mice. J. Gastroenterol. Hepatol. 2009; 24:1658–68. [PubMed: 19788606]

10. Silversand C, Haux C. Improved high-preformance liquid chromatographic method for the separation and quantification of lipid classes: application to fish lipids. J. Chromatogr. B. 1997; 703:7–14.

11. Kleiner DE, Brunt EM, Van Natta M, Behling C, Contos MJ, Cummings OW, Ferrell LD, Liu YC, Torbenson MS, Unalp-Arida A, Yeh M, McCullough AJ, Sanyal AJ. Design and validation of a histological scoring system for nonalcoholic fatty liver disease. Hepatology. 2005; 41:1313–21. [PubMed: 15915461]

12. Stone BG, Evans D, Prigge WF, Duane WC, Gebhard RL. Lovastatin treatment inhibits sterol synthesis and induces HMG-CoA reductase activity in mononuclear leukocytes of normal subjects. J. Lipid Res. 1989; 30:1943–1952. [PubMed: 2621421]

13. Clayton DF, Darnell JE Jr. Changes in liver-specific compared to common gene transcription during primary culture of mouse hepatocytes. Mol. Cell. Biol. 1983; 3:1552–61. [PubMed: 6633533]

14. Pandak WM, Li YC, Chiang JY, Studer EJ, Gurley EC, Heuman DM, Vlahcevic ZR, Hylemon PB. Regulation of cholesterol 7 alpha-hydroxylase mRNA and transcriptional activity by taurocholate and cholesterol in the chronic biliary diverted rat. J. Biol. Chem. 1991; 266:3416–21. [PubMed: 1995604]

15. Wu Z, Chiang JY. Transcriptional regulation of human oxysterol 7 alpha-hydroxylase gene (CYP7B1) by Sp1. Gene. 2001; 272:191–7. [PubMed: 11470525]

16. Twisk J, de Wit EC, Princen HM. Suppression of sterol 27-hydroxylase mRNA and transcriptional activity by bile acids in cultured rat hepatocytes. Biochem. J. 1995; 305(Pt 2):505–11. [PubMed: 7832767]

17. Zhang M, Chiang JY. Transcriptional regulation of the human sterol 12alpha-hydroxylase gene (CYP8B1): roles of heaptocyte nuclear factor 4alpha in mediating bile acid repression. J. Biol. Chem. 2001; 276:41690–9. [PubMed: 11535594]

18. del Castillo-Olivares A, Gil G. Role of FXR and FTF in bile acid-mediated suppression of cholesterol 7alpha-hydroxylase transcription. Nucleic Acids Res. 2000; 28:3587–93. [PubMed: 10982880]

19. Pagano G, Pacini G, Musso G, Gambino R, Mecca F, Depetris N, Cassader M, David E, Cavallo-Perin P, Rizzetto M. Nonalcoholic steatohepatitis, insulin resistance, and metabolic syndrome: further evidence for an etiologic association. Hepatology. 2002; 35:367–72. [PubMed: 11826410]

20. Wang L, Han Y, Kim CS, Lee YK, Moore DD. Resistance of SHP-null mice to bile acid-induced liver damage. J. Biol. Chem. 2003; 278:44475–81. [PubMed: 12933814]

21. Grassi A, Susca M, Ferri S, Gabusi E, D'Errico A, Farina G, Maccariello S, Zauli D, Bianchi FB, Ballardini G. Detection of the M30 neoepitope as a new tool to quantify liver apoptosis: timing and patterns of positivity on frozen and paraffin-embedded sections. Am. J. Clin. Pathol. 2004; 121:211–9. [PubMed: 14983934]

22. Adams LA, Feldstein A, Lindor KD, Angulo P. Nonalcoholic fatty liver disease among patients with hypothalamic and pituitary dysfunction. Hepatology. 2004; 39:909–14. [PubMed: 15057893]

23. Xie X, Liao H, Dang H, Pang W, Guan Y, Wang X, Shyy JY, Zhu Y, Sladek FM. Down-regulation of hepatic HNF4alpha gene expression during hyperinsulinemia via SREBPs. Mol. Endocrinol. 2009; 23:434–43. [PubMed: 19179483]

24. Lee YK, Schmidt DR, Cummins CL, Choi M, Peng L, Zhang Y, Goodwin B, Hammer RE, Mangelsdorf DJ, Kliewer SA. Liver receptor homolog-1 regulates bile acid homeostasis but is not essential for feedback regulation of bile acid synthesis. Mol. Endocrinol. 2008; 22:1345–1356. [PubMed: 18323469]

25. Lee YK, Choi YH, Chua S, Park YJ, Moore DD. Phosphorylation of the hinge domain of the nuclear hormone receptor LRH-1 stimulates transactivation. J. Biol. Chem. 2006; 281:7850–7855. [PubMed: 16439367]

26. Freeman LA, Kennedy A, Wu J, Bark S, Remaley AT, Santamarina-Fojo S, Brewer HB Jr. The orphan nuclear receptor LRH-1 activates the ABCG5/ABCG8 intergenic promoter. J. Lipid Res. 2004; 45:1197–1206. [PubMed: 15121760]

27. Song X, Kaimal R, Yan B, Deng R. Liver receptor homolog 1 transcriptionally regulates human bile salt export pump expression. J. Lipid Res. 2008; 49:973–84. [PubMed: 18270374]

28. Tabas I. Free cholesterol-induced cytotoxicity. A possible contributing factor to macrophage foam cell necrosis in advanced atherosclerotic lesions. Trends Cardiovasc. Med. 1997; 7:256–263. [PubMed: 21235894]

29. Ioannou GN, Morrow OB, Connole ML, Lee SP. Association between dietary nutrient composition and the incidence of cirrhosis or liver cancer in the United States population. Hepatology. 2009; 50:175–84. [PubMed: 19441103]
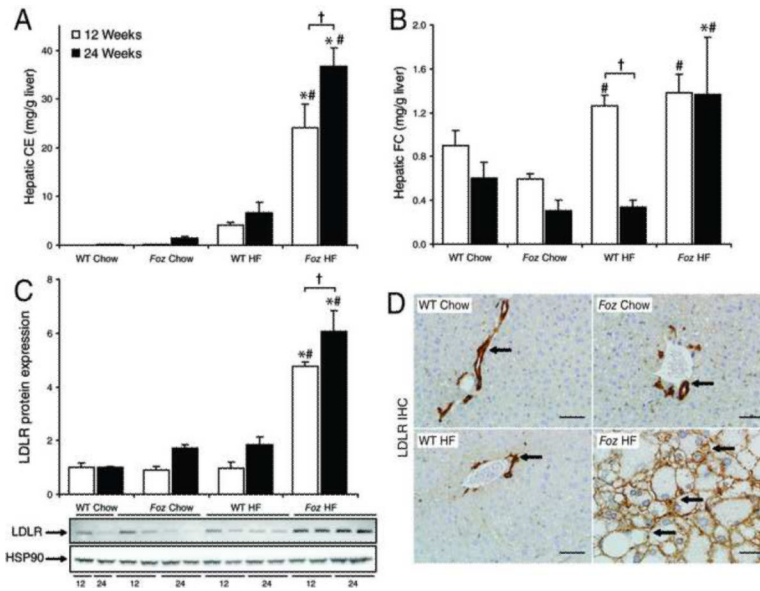
Figure 1. Increased hepatic cholesterol levels and LDLR expression in *foz/foz* mice with NASH
(*A*) Hepatic cholesteryl ester (CE) and (*B*) free cholesterol (FC) content in normal chow (0% [w/w] cholesterol) and HF (0.2% [w/w] cholesterol)-fed WT and *foz/foz* mice at 12- (□) and 24- (▪) weeks (*n*=5–10/grp – see METHODS) as determined by HPLC. (*C*) LDL receptor (LDLR) protein expression, normalized to heat-shock protein 90 (HSP90) expression. (*D*) Representative LDLR IHC staining from 24-week liver sections. Arrows indicate positive staining. Scale bars represent 50 μm. *P<0.05, vs. diet-matched control. #P<0.05, vs. genotype-matched control. †P<0.05, vs. time-matched control.
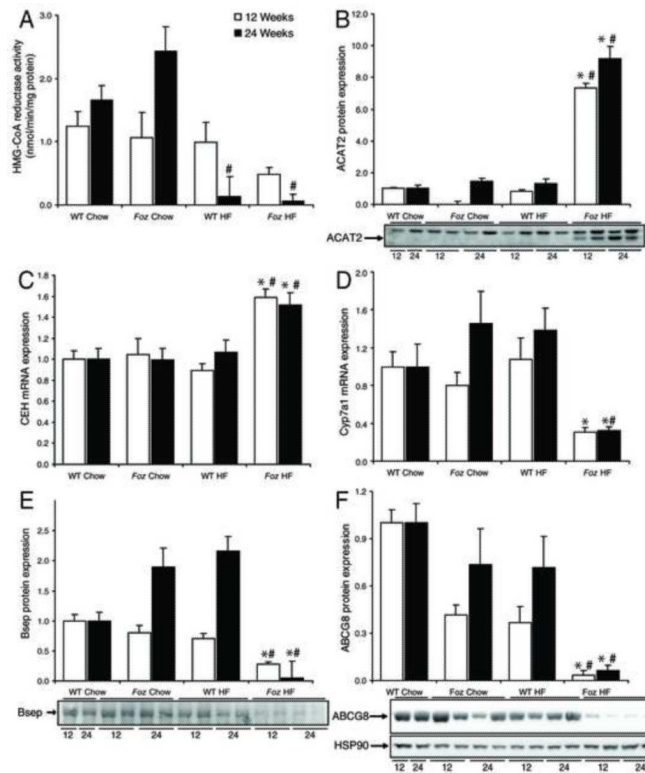
Figure 2. Decreased cholesterol and bile acid biosynthesis, and canalicular transporter gene expression in HF-fed *foz/foz* versus wildtype mice

(*A*) Microsomal HMG-CoA reductase activity at 12- (□) and 24-weeks (•) in *foz/foz* and WT mice according to diet (values for *n* are in METHODS). (*B*) Hepatic acyl-CoA:cholesterol acyltransferase (ACAT)-2 protein, (*C*) cholesteryl ester hydrolase (CEH) mRNA, and (*D*) Cyp7a1 mRNA expression at 12-and 24-weeks. (*E*) Hepatic bile salt exporter protein (Bsep) and (*F*) ATP-binding cassette protein-G8 (ABCG8) protein expression at 12- and 24-weeks. Heat shock protein-90 (HSP90) (shown in panel *F*) was used as a loading control, but not shown in all panels for clarity (results for loading controls were similar). Same mice as in Figure 1. *$P<0.05$, vs. diet-matched control. #$P<0.05$, vs. genotype-matched control. †$P<0.05$, vs. time-matched control.
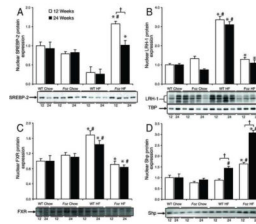
Figure 3. Effect of diet and genotype on hepatic expression of nuclear regulators involved in cholesterol homeostasis
(*A*) Sterol-response element binding protein-2 (SREBP-2), (*B*) liver-receptor homolog-1 (LRH-1), (*C*) farnesoid X-receptor (FXR), and (*D*) small heterodimer partner (Shp) expression at 12-(□) and 24- (▪) weeks was assessed using western blotting of isolated hepatic nuclear protein. TATA-box binding protein (TBP) (shown in panel *B*) was used as a loading control. Same mice as preceding figures. *$P<0.05$, vs. diet-matched control. #$P<0.05$, vs. genotype-matched control. †$P<0.05$, vs. time-matched control.
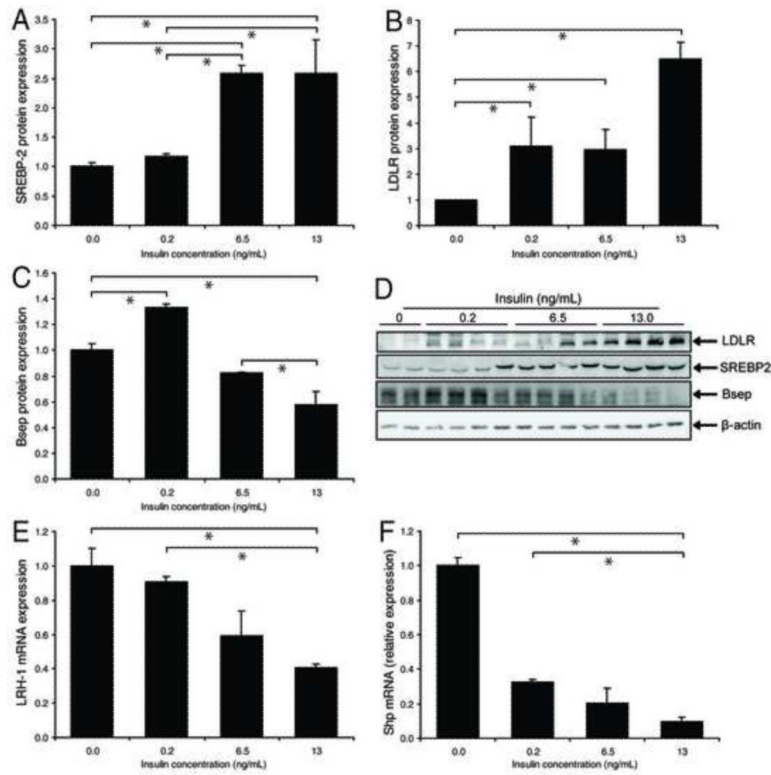
Figure 4. Insulin alters cholesterol-regulating protein expression in primary hepatocyte cultures
(*A*) Levels of sterol-response element binding protein-2 (SREBP-2), (*B*) low density
lipoprotein receptor (LDLR), and (*C*) bile salt exporter protein (Bsep) expression in primary
hepatocytes (whole cell lysates) treated with 0, 0.2, 6.5, and 13.0 ng/ml insulin for 48 h
(*n*=3/grp). As shown in (*D*), protein expression was normalised to β-actin. (*E*) Liver receptor
homolog-1 (LRH-1) and (*F*) small heterodimer partner (Shp) mRNA was assessed by RT-
PCR. There was insufficient material to prepare nuclear protein extracts. This experiment
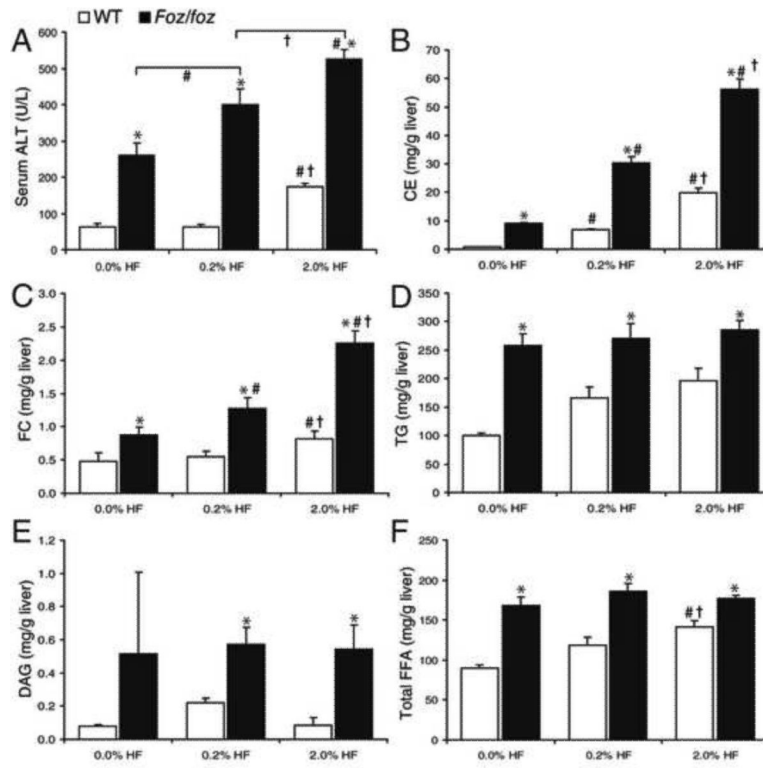was conducted three times with analyses in triplicate (*n*=9/grp total). *$P<0.05$ between
groups.

Figure 5. Dietary cholesterol modulates hepatic cholesterol content and liver injury, but not other lipid profiles in NASH

(*A*) Serum alanine transaminase (ALT), (*B*) total hepatic cholesteryl ester (CE), and (*C*) hepatic free cholesterol (FC) content in WT (□) and *foz/foz* (▪) mice (*n* values as per METHODS) fed HF-diet containing 0, 0.2 or 2.0% (w/w) cholesterol for 24-weeks. (*D*) Hepatic TG, (*E*) diacylglycerides (DAG), and (*F*) total free fatty acids (FFA), as determined by HPLC. *$P<0.05$, vs. diet-matched control. #$P<0.05$, vs. genotype-matched, 0.0% cholesterol groups. †$P<0.05$, vs. genotype-matched, 0.2% cholesterol groups
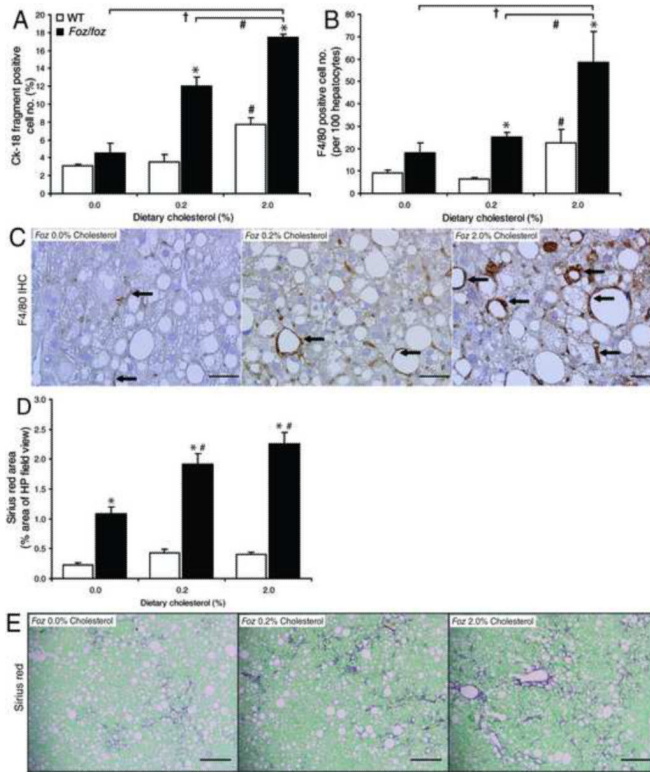
Figure 6. Dietary cholesterol modulates hepatocyte apoptosis and macrophage recruitment in NASH

(*A*) Cell death, as assessed by cytokeratin-18 (Ck-18) fragmentation, and (*B*) macrophage cell recruitment (F4/80) were determined using IHC detection to (*C*) quantify positive cells (methods). (D) Quantification (ImageJ) of representative Sirius red-stained liver sections (E) from WT (□) and *foz/foz* (▪) mice (*n* values as per METHODS) fed HF-diet containing 0, 0.2 or 2.0% (w/w) cholesterol for 24-weeks. Arrows indicate positive staining. Same livers as Figure 5. Scale bars represent 20 μm (panel *C*) and 500 μm (panels *E*). *P<0.05, vs. diet-matched control. #P<0.05, vs. genotype-matched, 0.2% cholesterol groups. †P<0.05, vs. genotype-matched, 2.0% cholesterol groups

Table 1

Effects of dietary cholesterol content on liver histology in *foz/foz* and WT mice fed HF diet or chow.

Genotype	WT			Foz/foz		
HF Diet	**0.0% FC**	**0.2% FC**	**2.0% FC**	**0.0% FC**	**0.2% FC**	**2.0% FC**
Steatosis	0.2 ± 0.1	0.1 ± 0.1	$0.4 \pm 0.2^{\dagger\#,*}$	$2.8 \pm 0.1^{\P}$	$2.9 \pm 0.0^{\P}$	$2.8 \pm 0.2^{\P}$
Inflammation	0.1 ± 0.1	$0.6 \pm 0.1^{\#,*}$	0.3 ± 0.3	0.7 ± 0.2	0.9 ± 0.2	1.1 ± 0.3
Ballooning	0	0.3 ± 0.0	0	0.3 ± 0.2	0.5 ± 0.1	$1.0 \pm 0.3^{\P,\#,*,\dagger}$
NAS	$0.3 \pm 0.2^{*}$	$0.1 \pm 0.2^{\#*}$	$0.7 \pm 0.4^{\dagger,\#,*}$	$3.9 \pm 0.2^{\P,*}$	$4.3 \pm 0.2^{\P\#,*}$	$4.8 \pm 0.3^{\P,\#,*,\dagger}$
NASH	0/8	0/9	0/8; 1 borderline	0/8	1/11; 10 borderline$^{\P,\#,*}$	6/7 NASH; 1 borderline$^{\P\#,*,\dagger}$

Data (mean±SEM; *n* is described in METHODS) represent histological scores for severity of steatosis, inflammation and ballooning, according to criteria of Kleiner *et at* (11), previously reported in this model (9). NAFLD activity score (NAS) and designation as NASH, borderline or not NASH was determined blind by an experienced liver histopathologist (MMY) according to published criteria (11).

* *P* < 0.05, compared to genotype-matched, chow control.

# *P*<0.05, compared to genotype-matched, 0.0% cholesterol-HF group.

† *P*<0.05, compared to genotype-matched, 0.2% cholesterol-HF group.

¶ *P*<0.05, compared to diet-matched, genotype control.